International Journal of Biological Macromolecules 216 (2022) 629–642

Contents lists available at ScienceDirect

International Journal of Biological Macromolecules

journal homepage: www.elsevier.com/locate/ijbiomac

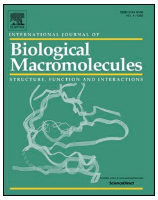

Emulsifying properties and bioavailability of clove essential oil Pickering emulsions stabilized by octadecylaminated carboxymethyl curdlan

Huan Li [a], Chuanchao Wu [a], Zhongwei Yin [a], Jianrong Wu [a], Li Zhu [b], Minjie Gao [a], Xiaobei Zhan [a,*]

[a] Key Laboratory of Carbohydrate Chemistry and Biotechnology of Ministry of Education, School of Biotechnology, Jiangnan University, Wuxi, Jiangsu 214122, China
[b] A & F Biotech. Ltd., Burnaby, BC V5A3P6, Canada

ARTICLE INFO

Keywords:
Pickering emulsion
Clove essential oil
Carboxymethyl curdlan

ABSTRACT

In the present study, clove essential oil (CEO) Pickering emulsions were stabilized by octadecylamine-modified carboxymethyl curdlan (CMCD-ODA) at different pH values. The droplet size and negatively charged zeta potential of the CMCD-ODA emulsions decreased as the pH increased from 3.0 to 11.0. Rheology results indicated that the CMCD-ODA polymer/emulsion prepared at pH 5.0 showed higher apparent viscosity and viscoelasticity than other pH conditions, which might prevent droplets from flocculating. The Pickering emulsions obtained at pH 5.0 were spherical droplets with a uniform size distribution and a mean diameter of 9.54 μm, and they exhibited excellent stability during 28 days of storage. The morphological structures of the emulsions investigated by confocal laser scanning microscopy and scanning electron microscopy indicated that the CMCD-ODA Pickering emulsion obtained at pH 5.0 was stabilized by loading amphiphilic CMCD-ODA polymer around the spherical oil droplets and forming a weak gel network structure. The CEO-loaded CMCD-ODA emulsions had higher antioxidant capacity than free CEO after 28 days of storage at pH 5.0. Given the good emulsion stability, antioxidant activity, and great antibacterial effect, the CEO-loaded carboxymethyl curdlan Pickering emulsion has promising applications in food, cosmetic, and biomedicine industries.

1. Introduction

Clove essential oil (CEO) contains several active components, such as eugenol and caryophyllene, which has been widely studied for their antioxidant, antimicrobial, anti-inflammatory, and other biological activities [1]. Thus, CEO is widely applied in food, cosmetic, pharmaceutical, and active packaging industries [2]. However, the practical application of CEO is strictly limited by its light sensitivity, volatilization, and low water solubility. Therefore, different encapsulation strategies, such as microcapsulation, microsphere, and nanoparticles, have been developed to address these problems [1].

Pickering emulsions, as a kind of emulsion stabilized by colloidal particles rather than traditional surfactants, have elicited extensive research interest in food, cosmetic, and pharmaceutical industries recently [3]. Unlike surfactants, Pickering emulsions have superior anti-flocculation and anti-coalescence properties, high evaporation resistance to volatile oils, good elastic responses due to the formation of close-packed layers on the oil/water (O/W) interface by colloidal particles, and allow for the formation of a dense three-dimensional network [4,5]. Amphiphilic polymers are used as "soft particles" in Pickering emulsions; these polymers can easily self-assemble or disassemble depending on the surrounding conditions and provide attractive characteristics for further utilization [6,7]. In particular, natural polymer emulsifiers are eliciting increased attention in emulsion-related fields due to their good biocompatibility [7].

Curdlan is a linear microbial exopolysaccharide bearing β-1,3-glucan with a triple-helix structure [8]. Curdlan is widely used as a safe food additive, gene/drug delivery carrier, and immune-stimulant in food, cosmetic, and biomedicine areas due to its unique gelling capability, biodegradability, biocompatibility, and strong bioactivity [9]. Carboxymethyl modification of curdlan exhibits beneficial biological activity (such as immunocompetence and antitumor activity) and excellent water solubility, thus providing attractive properties for further applications in health and biomedical fields [10]. In recent years, carboxymethyl curdlan (CMCD) has been used to prepare amphiphilic curdlan derivatives, and then self-assemble to deliver hydrophobic drugs or

---

* Corresponding author.
E-mail address: xbzhan@yahoo.com (X. Zhan).

https://doi.org/10.1016/j.ijbiomac.2022.07.029
Received 9 March 2022; Received in revised form 24 June 2022; Accepted 4 July 2022
Available online 8 July 2022

bioactive ingredients [11–13]. CMCD has also been employed as emulsion microspheres for protein adsorption [14]. However, limited research has been conducted on self-assembled CMCD particles as Pickering emulsifiers because of the poor solubility of CMCD in the oil phase. Therefore, amphiphilic CMCD polymers have been prepared through hydrophobicity modification to improve the stability of CEO emulsions.

N-octadecylamide-modified polysaccharides have an amphiphilic property associated with many biological activities, including antibacterial, analgesic, and anti-inflammatory effects, which are promising for the adsorption of cholesterol, fat, and other therapeutic agents [15]. For example, *N*-octadecylamides of carboxymethylcellulose have been used as lipid sorbents and cholesterol-lowering agents [16]. A previous study has shown that octadecylamine (ODA)-modified hyaluronic acid forms clearly defined hydrophobic domains for paclitaxel delivery [17]. *N*-octadecylpectinamide has also been applied as stabilizers of O/W emulsions [18]. Compared with these polysaccharides, curdlan, with its excellent biological activities, can be mass-produced by bacteria and can be potentially developed as a new emulsifier via octadecylamine modification.

In this study, an amphiphilic curdlan polymer was synthesized by grafting ODA on the surface of CMCD through an amidation reaction. CEO-loaded CMCD-ODA O/W Pickering emulsions were prepared at various pH values via homogenization. The effects of pH on the particle size, stability, and rheological property of the emulsions were investigated. The morphology of the Pickering emulsions and the antioxidant/antibacterial activities of the CEO emulsions were also evaluated.

2. Materials and methods

2.1. Materials

Curdlan (91 %, absolute molecular weight = 1.31×10^6 Da) was obtained from PT. Fermentech Indonesia (Lampung, Indonesia). Chloroacetic acid (99 %) and CEO were supplied by Sinopharm Chemical Reagent Co., Ltd. (Shanghai, China). ODA (96 %) was obtained from Beijing InnoChem Science & Technology Co., Ltd. (Beijing, China). N-(3-Dimethylaminopropyl)-N′-ethylcarbodiimide hydrochloride (98 %, EDC) and N-hydroxysuccinimide (98 %, NHS) were obtained from Shanghai Aladdin Bio-Chem Technology Co., Ltd. (Shanghai, China) together with 2,2-diphenyl-1-picrylhydrazyl (DPPH, Sigma-Aldrich, Germany). *Escherichia coli* ATCC-25922 and *Staphylococcus aureus* ATCC-6538 were preserved in our laboratory.

2.2. Gas chromatography-mass spectrometry (GC–MS)

The chemical composition CEO was identified as described in a previous study by using a GC–MS (Trace1310-TSQ 8000; Thermo Scientific, San Jose, CA, USA) with a Thermo TG-WAXMS capillary column (60 m × 0.25 mm × 0.25 μm) [19]. The components were confirmed by comparison of the obtained spectra with standard NIST2014 library, and the relative content of each component was obtained by calculating the relative percent peak area with the peak area normalisation method [20].

2.3. Modification of CMCD with octadecylamine

CMCD was prepared in accordance with the methods as described previously with some modifications [21]. The degree of carboxymethylation substitution of CMCD quantified by conductometric back titration was 0.95 [22]. Moreover, after dissolving CMCD in D_2O, the ^1H NMR spectrum of CMCD was obtained by an Advance III 400 Hz NMR spectrometer (Bruker, Switzerland) to verify its high carboxymethylation. The relative molecular weight of CMCD was 3.12×10^6 Da, which was measured by high-performance gel filtration chromatography (1525, Waters, Milford, USA) equipped with a 2410 differential refraction detector and an Ultrahydrogel™ Linear column (300 mm × 7.8 mm, Waters, Milford, USA). CMCD-ODA polymer was synthesized by amidation of CMCD and ODA under the catalysis of EDC/NHS [23]. In brief, CMCD (1.0 g) was dissolved in ultrapure water, and NHS (0.13 g) was added to the solution and stirred at 25 °C for 30 min. An equimolar amount of NHS with DEC was added to the suspension under magnetic stirring for 1 h. Then, ODA equimolar to EDC/NHS was dissolved in ethanol (10 mL) at 50 °C, and it was made to react with CMCD with continuous stirring overnight at 50 °C. Afterward, the reaction mixture was washed with 0.1 M HCl ethanol solution then with ethanol solution. For further purification, the precipitate was dissolved in ultrapure water and dialyzed (MWCO = 8000 – 14,000 Da) against ultrapure water for three days. Then, the CMCD-ODA conjugate was obtained by freeze-drying the dialyzed solution.

2.4. Characterization of CMCD-ODA polymer

The attenuated total reflectance–Fourier transform infrared (ATR-FTIR) spectra for curdlan, CMCD, CMCD-ODA, and ODA at 4000–500 cm^{-1} were acquired using an FTIR spectrophotometer (Nicolet NEXUS, Thermo, USA).

The solubility of the polymer was determined as described by Silva et al. [24]. CMCD-ODA polymer was dispersed in ultrapure water, and the pH value of the solution (1 mg/mL) was adjusted to 3.0, 5.0, 7.0, 9.0, and 11.0, respectively. Those suspensions were stirred for 12 h at 25 °C and centrifugated at 10,000 rpm for 15 min. Then, the supernatants were dried at 105 °C to calculate the solubility. The light transmittance of the polymer (1 mg/mL) at different pH values was determined according to Jiang et al. [25]. Briefly, the absorbance of CMCD-ODA polymer dispersions at different pH values was measured at 600 nm. Ultrapure water was used as a blank control, and the light transmittance was 100 % [26]. The water contact angles of CMCD-ODA polymer at different pH values were investigated by an OCA15EC micro optical contact angle measurement (Dataphysics Instruments, Germany) with a pendant drop method [25].

2.5. Preparation of CMCD-ODA-stabilized Pickering emulsions

In preliminary experiments, the effects of parameters such as the shear rate, shear time, CMCD-ODA concentration, and the volume ratio of the water phase to the oil phase of the emulsion at pH 5.0 were investigated by observing whether phase separation occurred after 24 h of storage at 25 °C. At the same time, the droplet size and uniformity of emulsions were observed under a microscope to optimize the preparation process of the emulsion. Finally, Pickering emulsions were prepared at various pH values via homogenization. Briefly, the CMCD-ODA dispersion aqueous solution (10 mg/mL) was prepared by dispersing CMCD-ODA polymer in ultrapure water under continuous stirring for 12 h at 25 °C to ensure complete dissolution and hydration [9]. Then, the solution's pH was adjusted to 3.0, 5.0, 7.0, 9.0, and 11.0. The O/W Pickering emulsion was produced by adding CEO (8 mL) to the CMCD-ODA solution (20 mL, 10 mg/mL). Afterward, the emulsions were formed by homogenizing the mixture at 14,000 rpm for 5 min by using a digital ULTRA-TURRAX® instrument (IKA T18, Germany) [5]. The emulsions were ice-coated to avoid temperature variations during this process.

2.6. Droplet size and zeta potential determination

A Mastersizer 3000 laser diffraction particle size analyzer (Malvern instruments, UK) was employed to determine the particle size of the CMCD-ODA polymers and the droplet size of the CEO-loaded CMCD-ODA emulsions by static light scattering (SLS) as a function of pH. The CMCD-ODA polymers/emulsions after the storage of different times were added to the sample pump containing ultrapure water, and the particles were suspended at a velocity of 2200 rpm with a refractive index of 1.466. Droplet size was expressed as volume-weighted average diameter ($D_{4,3}$) [27].

A Zetasizer Nano ZS90 instrument (Malvern Instruments, UK) was used to investigate the zeta potentials of the CMCD-ODA polymers and the CEO-loaded emulsions. Specifically, the CMCD-ODA water solution (7.14 mg/mL, approximately equivalent to the concentration of CMCD-ODA in the emulsion) or the freshly prepared emulsions were diluted 100 times with ultrapure water before measuring the zeta potential of the samples to avoid multiple scattering effects [9,28].

2.7. Rheological measurements

2.7.1. Steady shear rheology

The apparent viscosity and shear stress properties of the CMCD-ODA polymers/emulsions prepared at different pH values were tested using a MCR302 rheometer (Anton Paar, Austria) equipped with parallel plate geometry (plate diameter = 25 mm, gap size = 1 mm) at 25 °C [23]. The shear rate was in the range of 0.1–200 s^{-1}, and the obtained data were fitted with the Herschel–Bulkley model as follows [29]:

$$\sigma = \sigma_0 + K \cdot \gamma^n$$

where σ is the shear stress (Pa), σ_0 is the apparent yield stress (Pa), K is the consistency coefficient ($Pa \cdot s^n$), γ is the shear rate (s^{-1}), and n is the flow behavior index.

2.7.2. Dynamic viscoelastic measurements

All samples were initiated by first performing strain sweep (0.01 – 100 %) tests with a frequency fixed at 1 Hz to observe linear viscoelastic range [30]. Then, dynamic frequency sweeps were performed in the frequency range of 0.1 – 10 Hz with a fixed strain of 2 % to obtain the elastic modulus (G′) and viscous modulus (G″) results within the linear viscoelastic region [3].

2.8. Determination of emulsion stability

The CEO-loaded CMCD-ODA Pickering emulsions prepared at different pH values were placed in 10 mL glass tubes with screw caps. Then, the emulsions were stored for 3 h, 7 days, 14 days, and 28 days at 25 °C. The creaming index (CI) of the emulsions was calculated through the following equation in accordance with a previously reported method [31]:

$$\mathrm{CI}\ (\%) = (\mathrm{H_C}/\mathrm{H_T}) \times 100\%$$

where H_C is the height of the serum layer (clear liquid) and H_T is the total height of the emulsion.

2.9. Characterization of the emulsion microstructure

2.9.1. Confocal laser scanning microscope (CLSM)

The microstructures of the CMCD-ODA emulsions prepared at pH 5.0 were characterized through a CLSM (TCS SP8, Leica, Germany) as described by Huang et al. [32]. Dye (50 μL, consisting of 1 % Nile red and 0.1 % Nile blue) was added to the emulsions (1 mL) for internal oil phase (red) and CMCD-ODA polymer (green) straining, respectively. After diluted 10-fold with ultrapure water, the dyed emulsions (10 μL) were dropped on a glass slide and covered with a coverslip. Then, the CMCD-ODA emulsions were observed using CLSM with argon and helium neon lasers at excitation wavelengths of 488 and 633 nm, respectively.

2.9.2. Scanning electron microscope (SEM)

The surface morphology of the CMCD-ODA emulsions prepared at pH 5.0 was analyzed using SEM (FEI Quanta 200, FEI Company, Eindhoven, The Netherlands) in accordance with the oil-phase solidification method [33]. Azobisisobutyronitrile (AIBN) was used as the oil-soluble initiator to initiate the emulsion polymerizations of styrene. In brief, 8 mL of styrene containing AIBN (10 mg) was utilized as the oil phase to replace CEO, and mixed with 20 mL of CMCD-ODA (pH 5.0, 10 mg/mL) suspension continuous phase. The mixture was homogenized at 14,000 rpm for 5 min and then polymerized at 50 °C for 20 h [33]. Afterward, the emulsion was washed with ultrapure water and freeze-dried for SEM observation.

2.10. Antioxidant activity of CEO-loaded curdlan emulsions

The DPPH free radical scavenging method was used to determine the antioxidant activities of free CEO and CEO-loaded CMCD-ODA emulsions by adopting a Hitachi U-3900 spectrophotometer (Hitachi High-Tech., Tokyo, Japan) [2]. To investigate the effect of pH on the stability of CEO, CEO was dissolved in 50 % (v/v) ethanol aqueous solution to obtain 1 mg/mL CEO ethanol solution, and the pH of the solution was adjusted to 3.0, 5.0, 7.0, 9.0 and 11.0. The antioxidant capacity of CEO under various pH conditions was determined after sealed storage at 25 °C for different times. Similarly, the antioxidant capacity of emulsions prepared at different pH values was also determined after sealed storage at 25 °C for different times.

To investigate the effect of CEO concentration on the antioxidant capacity of emulsions, the emulsion was prepared at pH 5.0 according to the method of Section 2.5 and then diluted with ultrapure water to obtain dilutions containing different concentrations of CEO (0.1 – 1 mg/mL, the density of CEO was 1.05 g/mL). Those dilutions (100 μL) were mixed with 5 mL of 0.1 mM ethanol solutions of DPPH and incubated in a dark condition for 30 min. The absorbance values of the samples were determined at 517 nm. The DPPH radical scavenging activity was calculated using the equation:

$$\text{DPPH radical scavenging activity}\ (\%) = [(\mathrm{A_C} - \mathrm{A_T})/\mathrm{A_C}] \times 100\%$$

where A_C is the absorbance of control samples substituted with ultrapure water and A_T is the absorbance of the tested samples.

2.11. Antibacterial ability of CEO-loaded CMCD-ODA emulsions

The antibacterial performance of free CEO and CEO-loaded CMCD-ODA emulsions prepared at pH 5.0 was assessed based on disc diffusion assay [34]. In brief, 100 μL of bacterial suspension (1×10^7 CFU/mL) was spread on LB agar medium. Then, 20 μL of the CEO-loaded emulsions and the same amount of free CEO were added to the surface of a sterile filter paper (6.0 mm in diameter) with PBS only as the blank group. The strains were incubated for 24 h at 37 °C, and the inhibition zones of the samples were determined.

2.12. Statistical analysis

All tests were performed three times, and the data were recorded as mean ± standard deviations. The results were analyzed with SPSS Statistics 22.0 software by using one-way ANOVA and Duncan's tests at a significance level of 0.05.

3. Results and discussion

3.1. Composition of CEO

The volatile constituents of CEO were measured via GC–MS. Thirty volatile compounds were identified in the CEO shown in Table 1, and they accounted for 98.36 % of the total constituents. The main compounds, including eugenol (58.50 %) and *β*-caryophyllene (21.06 %), were significantly higher than the other components; this result was in line with previous data reported by Campelo et al. [35]. Eugenol, a phenolic compound, is the major bioactive component in clove oil and plays a major role in its antioxidant, antibacterial, anti-inflammatory,

Table 1
Volatile constituents of clove essential oil measured via GC–MS.

No.	Amount (%)	Retention time (min)	Component	Formula
1	58.50	39.18	Eugenol	97-53-0
2	21.06	42.24	β-Caryophyllene	87-44-5
3	6.70	43.69	α-Caryophyllene	6753-98-6
4	2.90	46.22	3-Allyl-6-methoxyphenyl acetate	1941-09-9
5	2.69	15.90	Benzocyclobutene	694-87-1
6	2.39	52.19	14-Hydroxycaryophyllene	50277-33-3
7	1.68	49.05	Caryophyllene oxide	1139-30-6
8	0.27	41.37	Isoeugenol	97-54-1
9	0.19	48.62	(−)-Humulene epoxide II	19888-34-7
10	0.18	41.64	(−)-Isocaryophyllene	118-65-0
11	0.65	46.14	δ-Cadinene	483-76-1
12	0.16	40.22	α-Copaene	3856-25-5
13	0.15	40.00	Aromandendrene	489-39-4
14	0.13	45.47	α-Muurolene	31983-22-9
15	0.09	26.83	Nonanal	124-19-6
16	0.08	44.52	(+)-Cyclosativene	22469-52-9
17	0.07	45.07	α-Selinene	473-13-2
18	0.07	48.51	Caryophyllenyl alcohol	913176-41-7
19	0.06	44.72	Isospathulenol	88395-46-4
20	0.06	49.63	Humulene epoxide I	19888-33-6
21	0.05	45.96	δ-Guaiene	3691-11-0
22	0.05	51.22	(+)-Epicubenol	19912-67-5
23	0.04	50.87	Humulenol-II	19888-00-7
24	0.03	41.05	Methyleugenol	93-15-2
25	0.02	47.29	α-calacorene	21391-99-1
26	0.02	44.01	Alloaromadendrene	25246-27-9
27	0.02	38.94	à-Cubebene	17699-14-8
28	0.02	31.57	Methyl salicylate	119-36-8
29	0.02	53.88	Spathulrnol	6750-60-3
30	0.02	26.64	Linalool	78-70-6

and anti-cancer properties [20,36]. Furthermore, other compounds, such as α-caryophyllene (6.70 %), 3-allyl-6-methoxyphenyl acetate (2.90 %), benzocyclobutene (2.69 %), 14-hydroxycaryophyllene (2.39 %), and caryophyllene oxide (1.68 %), were found in CEO (Table 1). CEO's chemical composition may be influenced by seasonal variations, drying and extraction methods, and the stages of plant growth [5]. This could explain the possible differences between the compound concentrations or compositions determined in the current research and the values obtained in other research.

3.2. Characterization of the CMCD-ODA derivative

The CMCD-ODA polymer was fabricated by hydrophobically modifying the primary –COOH groups on the CMCD surface. In preliminary experiments, the ratio of polar to non-polar groups was optimized by changing the degree of substitution in the carboxymethylated and amidation reactions, thus making amidated CMCD-ODA suitable for the stabilization of Pickering emulsions. Carboxymethylation with a high degree of substitution (0.95) was beneficial for unreacted carboxyl groups to maintain solubility and the pH responsiveness of the polymer after the esterification of some carboxyl groups (0.3 M) with amino groups (0.3 M). In the present study, carboxymethylation with a high degree of substitution (0.95) was performed to successively convert the C6, C2, and C4-primary hydroxyl groups in the triple-helix crystalline structure of native curdlan to a highly dissociable amorphous CMCD single-stranded chain containing carboxylate groups [37]. The structure of CMCD was confirmed via ^{1}H NMR (Fig. 1C). The peak of CMCD in the range of 3.0 – 3.9 ppm was due to the proton signals of anhydroglucose units. The signals in the range of 4.0 – 4.4 ppm were attributed to the protons from carboxymethyl groups at C6, C2, and C4 [37], indicating a successful synthesis of carboxymethylated curdlan with high degree of substitution. Afterward, the amphiphilic CMCD-ODA polymer was synthesized via covalent bonding with the –COOH groups of CMCD and the –NH_2 groups of ODA through EDC/NHS activation [17] (Fig. 1A). A schematic of the formation of the CEO-loaded CMCD-ODA O/W Pickering emulsion was displayed in Fig. 1B. CMCD-ODA could be anchored onto the O/W interface via the affinity of its alkyl chain groups to the oil phase, leading to the formation of closed packing layers around the oil droplets. In addition, the Pickering emulsion droplets were connected by the molecular backbone of CMCD-ODA, resulting in a gel-like network. Furthermore, the negative charge of the carboxylic groups (COO^-) of CMCD-ODA could provide strong electrostatic repulsion for inhibiting droplet flocculation. Therefore, the closed-layer, gel-like network and the electrostatic repulsion at the O/W interface helped improve the stability of the CEO-loaded CMCD-ODA Pickering emulsions.

As shown in the FTIR spectrum of CMCD (Fig. 1D), the adsorption peak at 3304 cm^{-1} corresponded to the stretching vibration of –OH and –COOH groups. After carboxymethylation, a new peak at 1588 cm^{-1} were attributed to the stretching vibration of the –COOH group, and the peak at 1414 cm^{-1} representing the symmetric vibration of the carboxymethyl group was significantly strengthened, which indicated that the CMCD was successfully synthesized [13]. Compared with the spectrum of CMCD, the absorption peak of CMCD-ODA at about 2900 cm^{-1} corresponding to the stretching vibration of –CH_3 and –CH_2 of ODA became double peaks (2914 indicating antisymmetric stretching and 2850 relating to symmetric stretching [16]). The intensity of the double peaks was obviously enhanced after ODA modification, indicating that ODA was successfully introduced into the structure of CMCD [17,38]. The characteristic band at 1730 cm^{-1} corresponded to the stretching vibration of the C=O of carboxyls and esters of CMCD-ODA [15].

As the pH increased from 3.0 to 11.0 (Fig. 2B), the solubility and light transmittance of the CMCD-ODA polymer solution increased significantly ($p < 0.05$) from 48.58 % to 87.42 %, and from 18.47 % to 70.09 %, respectively. The small solubility of the CMCD-ODA polymer at pH 3.0 was also confirmed by the opalescent appearance of the polymer solution (1 mg/mL) at pH 3.0 in Fig. 2A. On the contrary, at pH 11.0, the CMCD-ODA solution presented clear dispersions. Since Pickering emulsions were stabilized by insoluble particles, the incompletely water-soluble amphiphilic CMCD-ODA polymer would facilitate the formation of Pickering emulsions [39]. In addition, the CMCD-ODA dispersions at pH 5.0 with high polymer concentrations (10 mg/mL) could form weak gels (Fig. 2A). This phenomenon was also found in carboxymethyl cellulose sodium [40].

The water contact angles of CMCD-ODA polymer at different pH values were determined (Fig. 2C). The water contact angles decreased from 133.80° to 60.28° as the pH value increased from 3.0 to 11.0, indicating the lower surface hydrophobicity of the amphiphilic polymer under alkaline conditions. This was consistent with the trend of the contact angle of soybean fiber as a function of pH [41]. The aggregation of hydrophilic curdlan chains at pH 3.0 might lead to more exposure of hydrophobic chains, resulting in a greater hydrophobicity and a larger contact angle at pH 3.0 [25]. Interestingly, the contact angle of CMCD-ODA polymer at pH 5.0 was 93.93°, indicating the amphiphilic polymer at pH 5.0 possessed a near-neutral and preferable wettability. The water contact angle of CMCD-ODA polymer at pH 5.0 was closed to 90°, which could facilitate the effective adsorption of the polymer on the O/W interface [28], and improve the stability of CEO emulsions. Thus, CMCD-ODA polymer at pH 5.0 might be suitable for stabilizing the Pickering emulsions.

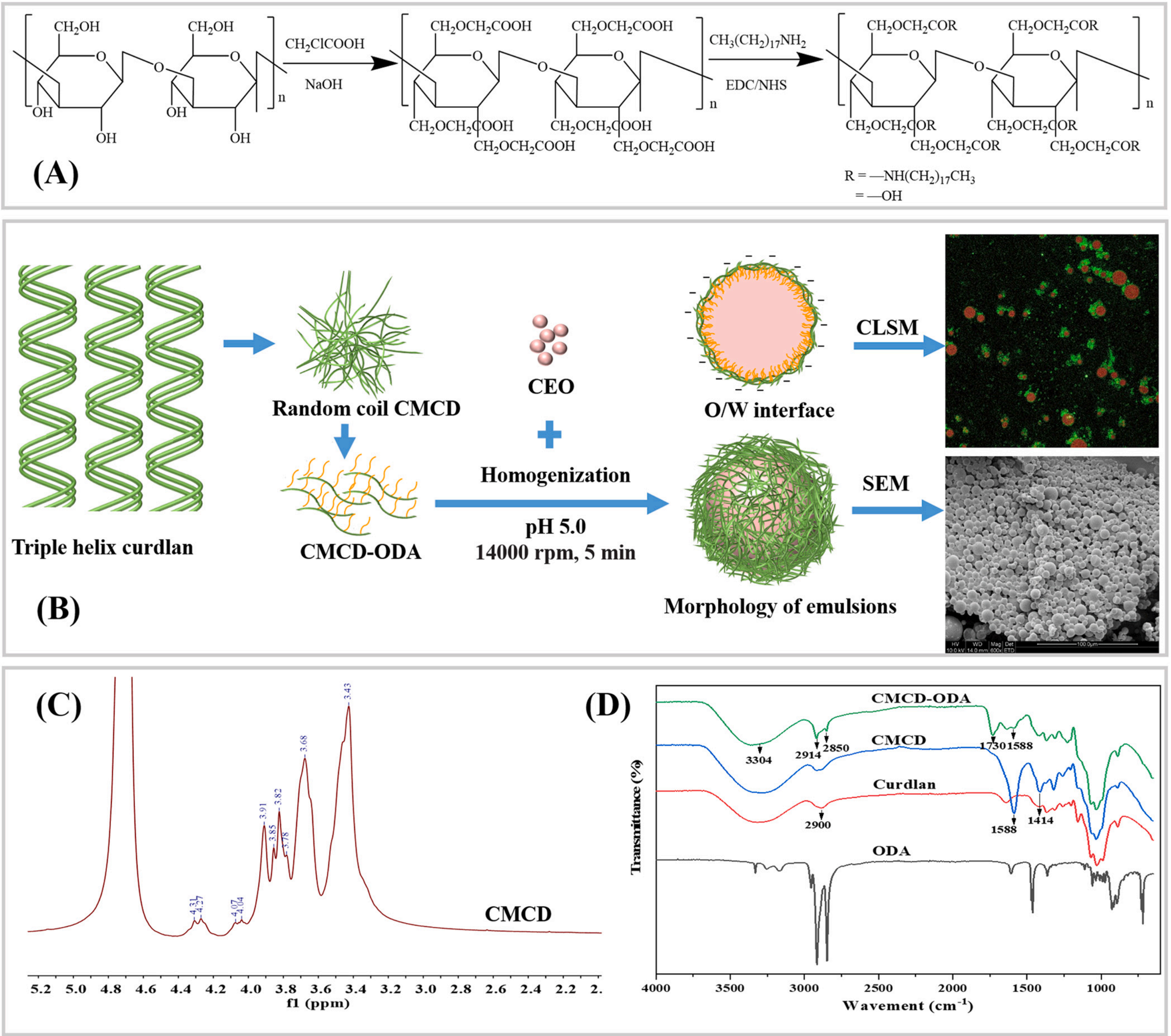

Fig. 1. (A) Synthetic scheme of CMCD-ODA derivatives. (B) Proposed schematic of the formation of CEO-loaded CMCD-ODA emulsions. (C) ^{1}H NMR spectrum of the carboxymethyl curdlan. (D) FTIR spectra of the octadecylamine, curdlan, carboxymethyl curdlan and octadecylamine-modified amphiphilic curdlan polymers.

3.3. Droplet size and zeta potential

The droplet size/zeta potential of the amphiphilic CMCD-ODA polymers and CEO-loaded modified curdlan emulsions obtained at various pH values after the storage of different times are shown in Figs. 3A-D. pH exerted a considerable effect on the size and zeta potential of the CMCD-ODA polymers/Pickering emulsions, which decreased as the pH increased at 3 h of storage. After 3 h of storage, the particle size of the CMCD-ODA polymers decreased from 62.86 μm to 24.00 μm with the increasing pH values (Fig. 3A). The increased particle size of CMCD-ODA polymer at pH 3.0 was confirmed by the increased zeta potential at pH 3.0 (−2.98 mV), which was caused by the weakened electrostatic repulsion force and intensive van der Waals attractive force between particles [3]. The clumping and agglomeration of polymers led to the increased particle size [42], which was also consistent with solubility and transmittance results (Fig. 2B). Coincidentally, the minimum particle size of the polymer at pH 11.0 was 24.00 μm, which was consistent with the increased solubility (87.42 %) and large absolute zeta potential (61.60 mV) of the polymer at pH 11.0. The result implied that the enhanced electrostatic repulsion allowed the CMCD-ODA chains to be uniformly dispersed in the solution.

After 28 days of storage, no obvious change in the particle size/zeta potential of the polymer at pH 5.0, 7.0, and 9.0 was found (Fig. 3A and C), indicating that the polymer was stable at those pH conditions. However, the zeta potential value of the polymer at pH 3.0 decreased after 28 days of storage, which was due to the swelling degradation of the aggregates in the solution. Conversely, the zeta potential of the polymer at pH 11.0 increased slightly after 28 days of storage, probably due to the presence of Na^+ ions reducing the electrostatic repulsion between particles [43].

As for CMCD-ODA emulsions, after 3 h of storage, the droplet size of the emulsions (1.19 – 56.36 μm) at pH 3.0 – 11.0 was significantly lower than that of the polymers (Fig. 3B).The tangled molecular chains of the polymer were dispersed after homogenization and reassembled with the CEO, forming small emulsion droplets. After 3 h of storage, the droplet size of the emulsion increased with the decreasing pH values. At pH 11.0, the $D_{(4,3)}$ of the Pickering emulsion reached the minimum value of 1.19 μm, but increased remarkably at pH 3.0 (56.36 μm). The droplet

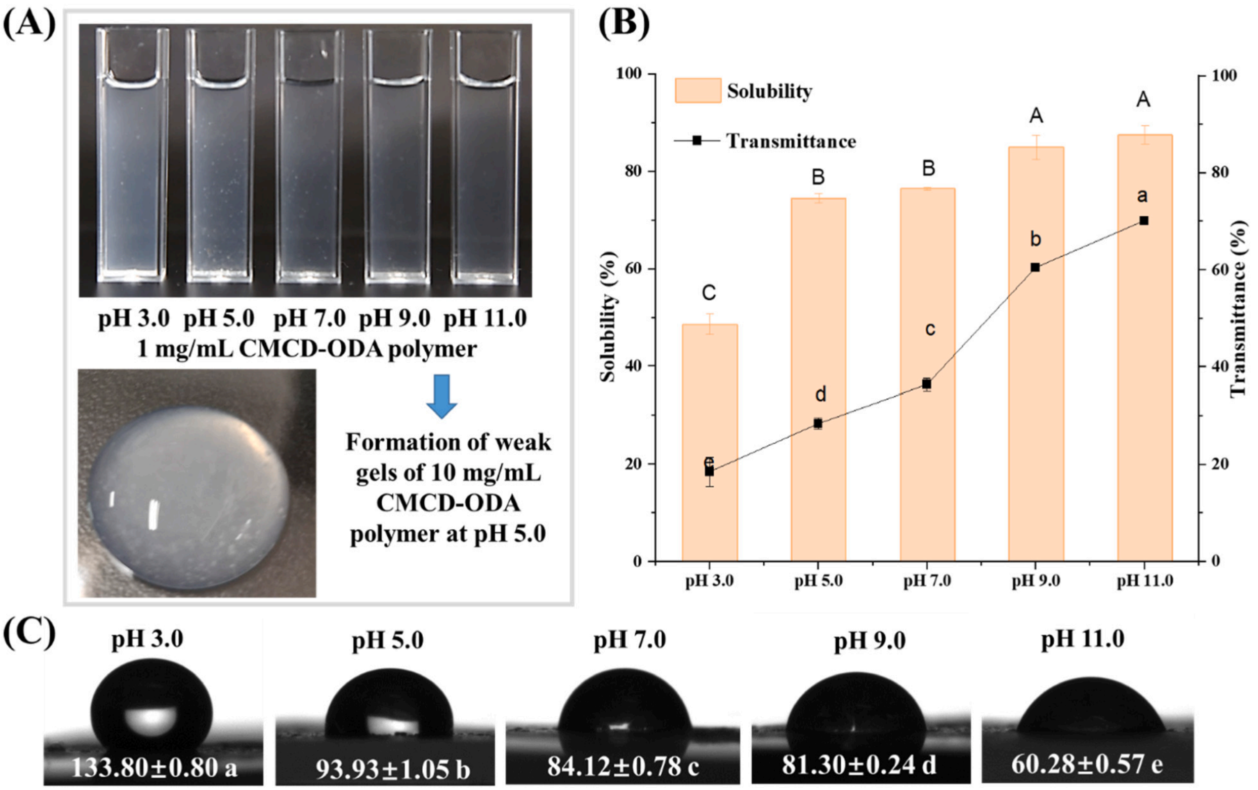

Fig. 2. (A) Appearance of the CMCD-ODA polymers at different pH conditions. (B) Solubility and light transmittance of polymers under different pH conditions. (C) Water contact angle of the CMCD-ODA polymer as a function of pH. Different capital and lower case letters within the bars indicate significant differences ($p < 0.05$) for solubility or transmittance, respectively.

size of the emulsion obtained at pH 11.0 was the smallest probably caused by the reduced viscosity of the CMCD-ODA continuous phase, which led to the improvement of homogenization efficiency during the preparation of the emulsion and the reduction of droplet size [4]. The $D_{(4,3)}$ of the CMCD-ODA emulsion was 9.54 and 4.49 μm for the emulsion prepared at pH 5.0 and 7.0, respectively, similar to the droplet size of the emulsion stabilized by ferulic acid-grafted curdlan (5.22 μm) [9].

The droplet size distributions of emulsions after the storage of different times were also shown in Fig. 3E and F. As shown in Fig. 3E, after 3 h of storage, the droplet size distribution of emulsions obtained at pH 5.0, 7.0, and 9.0 was relatively uniform, whereas the emulsions obtained at pH 3.0 or pH 11.0 presented multimodal distributions. After 28 days of storage, compared to the initial droplet size of emulsions (after 3 h of storage), the droplet size at pH 5.0 slightly increased with a relatively uniform unimodal distribution, while the droplet size of emulsions at other pH values significantly increased with wide range of multimodal distributions (Fig. 3F). This change might be related to the aggregation and precipitation between the emulsion droplets during the storage, depositing into large droplets [42].

The zeta potentials of the emulsion droplets obtained at various pH values were measured to quantify the intensity of the electrostatic interactions between emulsion droplets (Fig. 3D). As the pH increased from 3.0 to 11.0, the zeta potential of the CMCD-ODA emulsion decreased significantly ($p < 0.05$) with a range of −55.03 mV to −11.90 mV. The zeta potential was positively correlated with droplet size. The CMCD-ODA emulsions obtained at pH 3.0 showed the lowest negative zeta potential (−11.90 mV) probably due to the protonation of the carboxyl groups on the CMCD-ODA adsorbed on the emulsion interface [13]. Under the strong acid conditions, the low charge electrostatic repulsion between emulsions might have led to molecular entanglement and aggregation, resulting in the largest droplet size at pH 3.0 [27,30]. Conversely, the CMCD-ODA emulsion at pH 11.0 exhibited the highest negative charge (−55.03 mV) because of the deprotonation of carboxyl groups in CMCD-ODA, and the solubility of CMCD-ODA increased with increasing pH values, resulting in a reduced droplet size. The absolute zeta potential of emulsions at pH 9.0 and 11.0 became smaller after 28 days of storage. Due to the poor stability of the emulsion at pH 9.0/11.0, the bridging between droplets formed static electricity, which reduced the absolute potential value of the system [42]. However, the droplet size and zeta potential of the polymer or emulsion at pH 5.0 did not change significantly after 28 days of storage, suggesting that the emulsion exhibited good stability at pH 5.0.

These results demonstrated that the protonation-deprotonation process of carboxyl groups in CMCD-ODA was controlled by pH, which affected the charge density/droplet size of the emulsions, and was critical to the stability of the emulsions. However, the zeta potential alone without the other influential parameters could not predict the stability of the emulsion [44]. Generally, the stability of emulsion systems can be improved by electrostatic interactions between particles, but an excessive charge density adversely affects the particle adsorption at the O/W interface [27]. Thus, the stabilization mechanism of the CMCD-ODA emulsions was investigated via rheological determination.

3.4. *Rheological analysis of CEO-loaded CMCD-ODA emulsions*

The study of the rheology is an important method to provide useful information on the stability and internal microstructure of O/W emulsions [44]. Rheological viscosity is directly related to fluid stability and influences the suitability of emulsion processing [19]. The steady and dynamic shear rheology properties of the CMCD-ODA emulsions prepared at various pH values were investigated to further understand the effect of pH on emulsion performance.

3.4.1. *Steady shear rheology*

As shown in Fig. 4A-B, the apparent viscosities of the CMCD-ODA polymers and emulsions obtained at different pH values gradually

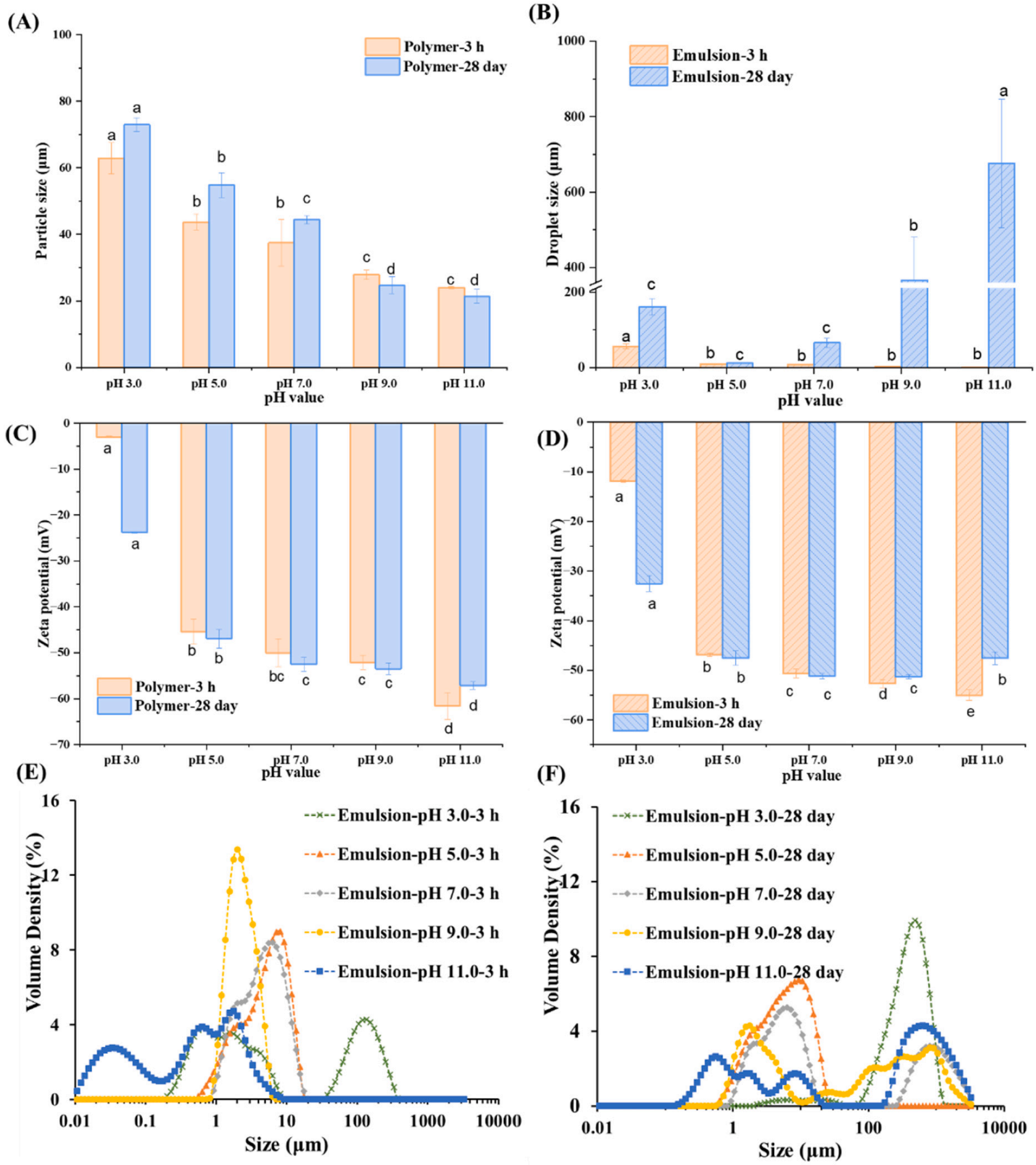

Fig. 3. Droplet size of (A) CMCD-ODA polymers and (B) emulsions at various pH values after storage at 25 °C for different times (3 h/28 days). Zeta potential of (C) CMCD-ODA polymers and (D) emulsions at various pH values after storage at 25 °C for different times (3 h – 28 days). The droplet size distribution of the emulsions obtained at pH 3.0–11.0 after storage for 3 h (E) and 28 days (F). The different letters in the bars indicate significant differences ($p < 0.05$) in particle size or zeta potential between different pH samples at the same storage time, respectively.

decreased when the shear rate ranged from 0.1 s^{-1} to 200 s^{-1}. The viscosity of the CMCD-ODA polymer first increased and then decreased with the increasing pH values, and the viscosity of the polymer was the highest at pH 5.0. As the pH increased from 3.0 to 5.0, the enhanced viscosity was due to the increased solubility, the enhanced electrostatic repulsion, and the formation of a weak gel by the swelled polymer at pH 5.0 [45,46].When the pH value of the system was higher than 5.0, the viscosity of the polymer decreased with the increase in pH values. With the increasing pH, carboxymethyl groups of CMCD-ODA were ionized, leading to an increased electrostatic repulsion. Then, the molecular chain of CMCD-ODA gradually expanded, resulting in a loose network structure and a decreased viscosity under alkaline conditions [47].

From Fig. 4B, the viscosity of CEO-loaded emulsion obtained at pH 5.0 was lower than the CMCD-ODA polymer, whereas the viscosities of emulsion prepared at other pH conditions were higher than the polymer at the same pH conditions. The viscosity of the emulsion at pH 5.0 was lower than that of the polymer, probably due to the high-speed shearing during the homogenization of the mixture of polymer and CEO, which might destroy some molecular weight hydrogen bonds, leading to a slightly decreased viscosity of the emulsion. However, at other pH conditions, the addition of CEO to the CMCD-ODA polymer with low viscosity might enhance the intermolecular forces of compounds in emulsion, resulting in an increased viscosity of emulsion [48].

The Herschel-Bulkley model was used to fit the steady shear rheology

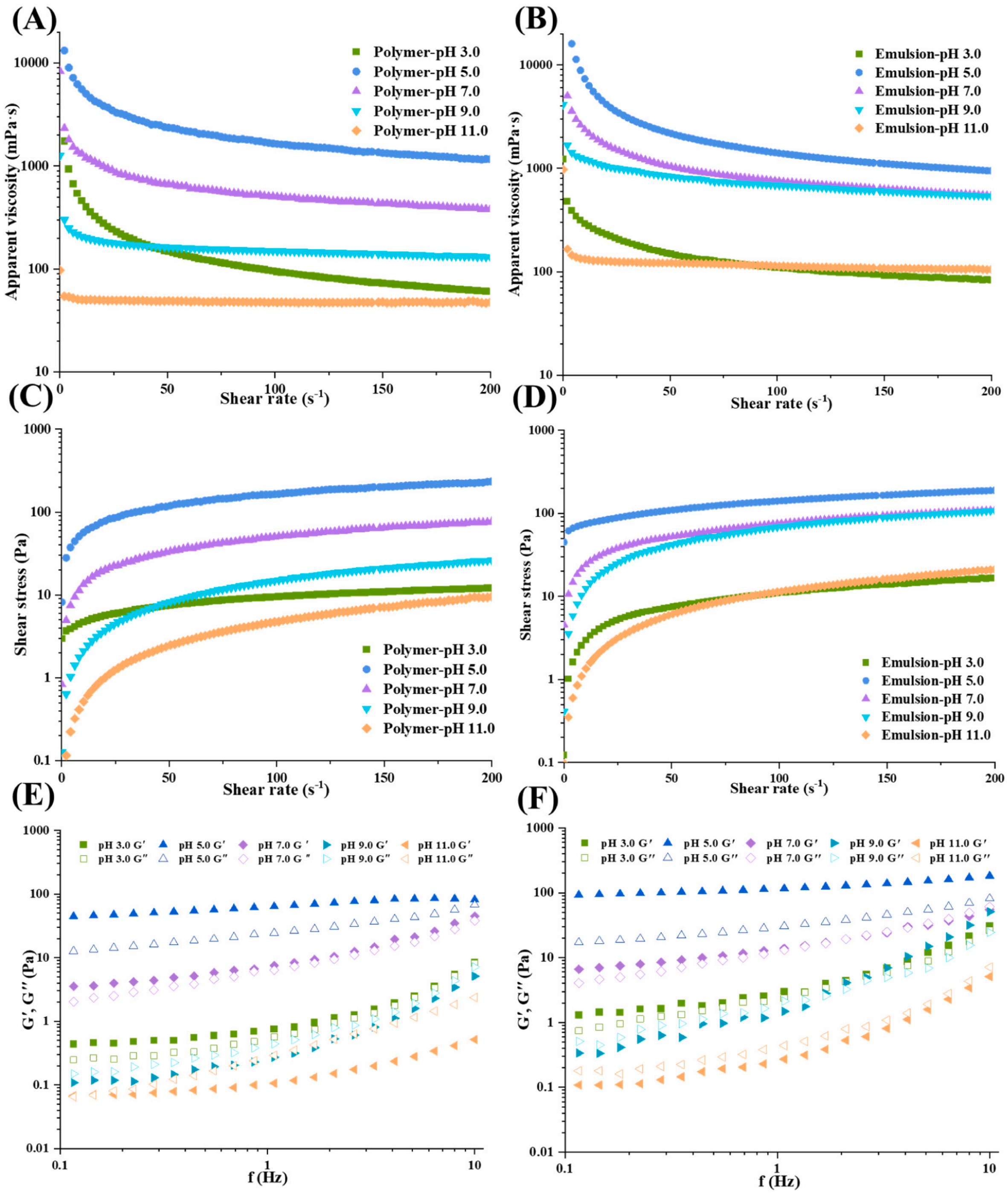

Fig. 4. (A/B) Apparent viscosity and (C/D) shear stress as a function of shear rate for CMCD-ODA polymers/emulsions obtained at various pH values. Storage modulus G′ and loss modulus G″ as a function of frequency sweep for (E) CMCD-ODA polymers and (F) emulsions.

Table 2
Experimental data of the CMCD-ODA polymer and the CEO-loaded CMCD-ODA emulsions obtained using the Herschel-Bulkley model.

pH values	σ_0 (Pa)		K (Pa.s^n)		n		R^2	
	polymer	emulsion	polymer	emulsion	polymer	emulsion	polymer	emulsion
3.0	2.36 ± 0.06	0.11 ± 0.08	0.81 ± 0.03	0.76 ± 0.03	0.47 ± 0.006	0.58 ± 0.006	0.998	0.999
5.0	1.93 ± 1.03	50.44 ± 0.61	17.77 ± 0.45	5.44 ± 0.18	0.48 ± 0.004	0.61 ± 0.006	0.999	0.999
7.0	0.45 ± 0.27	3.70 ± 0.40	3.08 ± 0.08	5.48 ± 0.14	0.61 ± 0.004	0.56 ± 0.004	0.999	0.999
9.0	0.00 ± 0.09	0.00 ± 0.73	0.34 ± 0.01	3.27 ± 0.18	0.82 ± 0.007	0.66 ± 0.009	0.999	0.998
11.0	0.06 ± 0.02	0.00 ± 0.05	0.05 ± 0.01	0.19 ± 0.01	1.00 ± 0.006	0.88 ± 0.005	0.999	0.999

Note: σ_0 is the apparent yield stress (Pa), K is the consistency coefficient (Pa·s^n), n is the flow behavior index, and R^2 is the correlation coefficient.

results in Fig. 4C-D and the fitted data are given in Table 2. The correlation coefficient (R^2) was higher than 0.998, signifying that the Herschel–Bulkley model fitted well with the rheological data in this study. The flow behavior index (*n*) of all samples was < 1.0, demonstrating that the emulsion displayed the behavior of shear thinning non-Newtonian fluid, which was pseudoplastic [31]. The shear-thinning flow behavior can be interpreted as the disruption of the formed entangled polymer network during the shearing process because of the breakage of the bridge connecting the emulsion droplets and the untangling of long-chain polymers [29]. In addition, when the destruction rate of intermolecular entanglement was greater than that of recombination at high shear rates, the intermolecular flow resistance and viscosity of the emulsions decreased [9]. The reduction of viscosity with increasing shear rate has also been observed in cellulose-based Pickering emulsions [23]. In particular, the highest consistency coefficient (*K*) value (17.77) for the polymer at pH 5.0 was in agreement with the largest viscosity at pH 5.0 presented in Fig. 4A. The viscosity of the polymer at pH 11.0 ($K = 0.05$) was significantly lower than those prepared at other pH conditions. In addition, the low *n* values for the polymer at pH 5.0 ($n = 0.48$) confirmed the strong shear-thinning behavior. In this study, the highest apparent viscosity of CMCD-ODA polymer at pH 5.0 might prevent droplets from flocculating [47], which could be verified by the emulsion stability results.

3.4.2. Dynamic shear properties

Dynamic frequency sweeps of the CMCD-ODA polymers and emulsions obtained at various pH values were carried out. According to Fig. 4E, the elastic modulus (G′) of the CMCD-ODA polymers at some pH conditions (pH 3.0, 5.0 and 7.0) was larger than the viscous modulus (G″). The elastic behavior dominated over the viscous behavior, suggesting an elastic gel-like structure in the CMCD-ODA polymers at pH 3.0, 5.0 and 7.0 [29]. Moreover, the G′ and G″ of the polymer exhibited frequency dependence over the entire sweep range, indicating that the formation of gel-like networks was mainly caused by non-covalent physical interactions [49]. Besides, the amphiphilic carrier material CMCD-ODA was highly aggregated at pH 3.0 but most polymer dissolved at pH 9.0 and 11.0, resulting in an unstable system at pH 3.0, 9.0 and 11.0.

The change trends of G′ and G″ of the emulsions as a function of pH were consistent with those of the polymers. As shown in Fig. 4F, the presence of CEO in the emulsions slightly increased the G' and G″. This result indicated that the CMCD-ODA polymer incorporating CEO could create stronger intermolecular interactions in emulsions, resulting in greater strength of the CMCD-ODA gel structure [48]. The G′ and G″ of the emulsions (at pH 3.0, 9.0, and 11.0) were significantly lower than that of other emulsions. At pH 9.0 and 11.0, G′ was slightly lower than G″, indicating a liquid-like behavior. A transition from well-formed gel behavior to solution-like behavior with increasing pH was also observed in carboxymethyl cellulose [40]. Particularly, the CMCD-ODA emulsions obtained at pH 5.0 showed a relatively higher viscoelastic modulus than the emulsions at other pH values, indicating the formation of a stronger elastic network structure at pH 5.0. Furthermore, the decreased charge density of CMCD-ODA at pH 5.0 facilitated interchain associations and increased the gel strength, resulting in gel formation. These results suggest that pH could modulate the viscosity and the viscoelasticity of emulsions, thus influencing the stability of the emulsions.

3.5. Stability of CMCD-ODA Pickering emulsions

Emulsion stability is influenced by the structure of molecules and the intermolecular interaction [50]. To evaluate the effect of pH on the stability of the emulsions stabilized by CMCD-ODA polymer, the appearance, optical microscopic images, and CI of the emulsions prepared at various pH values (3.0 – 11.0) after different storage times (3 h – 28 days) were investigated. As can be observed from the appearance of emulsions shown in Fig. 5, the pH values significantly affected the formation and subsequent stability of the CMCD-ODA emulsions. At 3 h of storage, obvious phase separation occurred in the emulsions prepared at pH 3.0. The upper layer comprised a transparent continuous phase, and the cream layer was located in lower layer (Fig. 5), which may be due to droplet coalescence during storage [47]. The emulsions obtained at pH 5.0 – 11.0 were stable after storage at 25 °C for 3 h, and no apparent differences were observed among them. Particularly, the CMCD-ODA emulsions displayed good interface stability at pH 5.0 aqueous medium during 28 days of storage. However, different degrees of destabilization and separation were found in the CMCD-ODA emulsions prepared at other pH values after 28 days of storage. After 28 days of storage, the emulsions prepared at pH 9.0 and 11.0 showed obvious phase separation, which was due to the poor hydrophobicity of the polymer under alkaline conditions (Fig. 2C), resulting in the release of some oil droplets from the emulsions. Finally, some brown oil droplets were deposited in the lower layer of the emulsion because of the large density of the CEO and the tendency to deteriorate under strong alkali conditions.

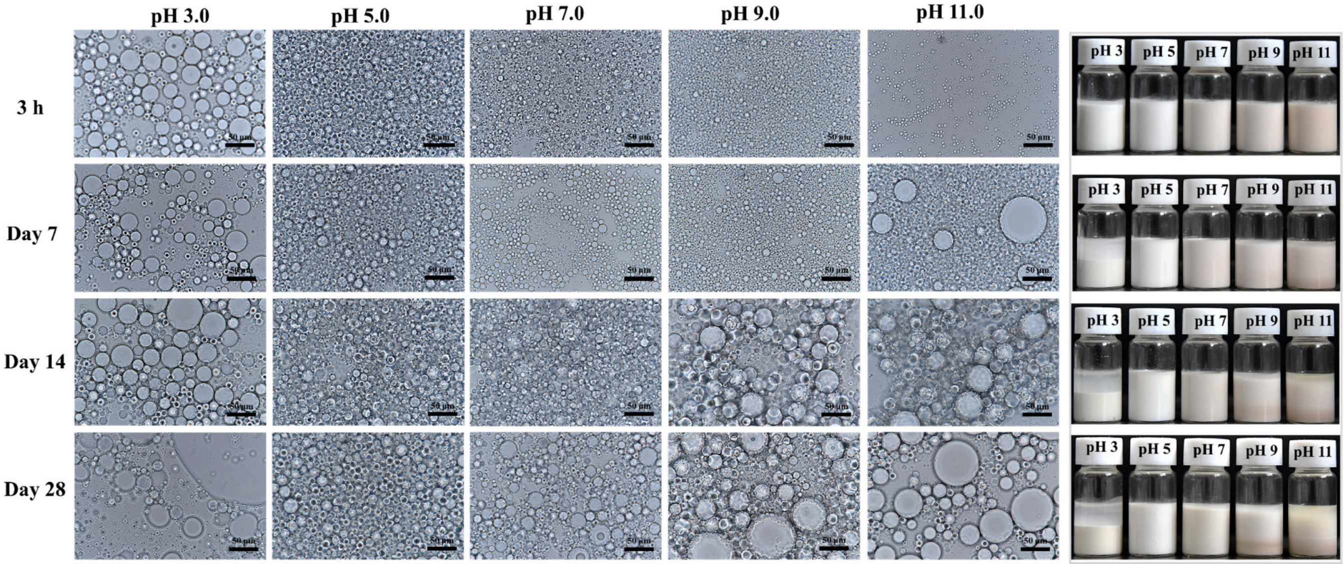

Fig. 5. Optical images and appearance of CEO-loaded CMCD-ODA emulsions prepared at different pH values after storage at 25 °C for different times (3 h – 28 days).

Light microscopic images of the Pickering emulsion stabilized by CMCD-ODA at different pH values were displayed in Fig. 5. The droplet size of the emulsion decreased with increasing pH in the first 3 h of storage, which was in agreement with the SLS results. The droplet size of the emulsion prepared under strong acid (pH 3.0) conditions was significantly larger than that of other emulsions at 3 h of storage. After storage for 7 days, the microscopic morphology of the emulsions at pH 5.0 – 9.0 showed no obvious change. The emulsion obtained at pH 11.0 was unstable after 7 days of storage, and the size of the emulsion droplets obtained at pH 11.0 became irregularly gathered probably due to the decreased viscosity and the poor hydrophobicity of the CMCD-ODA polymer under strongly alkaline conditions [4]. The emulsion prepared at pH 5.0 showed a uniform size distribution, and the droplet size did not change significantly after 28 days of storage, indicating that its stability was better than that of the others. Those results were consistent with the droplet size distribution determined by SLS (Fig. 3E – F).

CI, which indicated the degree of aggregation or separation of oil droplets during storage, was applied to measure the stability of the emulsions during long-term storage [32]. The smaller the CI value is, the more stable the system is [51]. The CIs of the different emulsions at various pH values are presented in Table 3. After 3 h of storage, the CI of all the emulsions was 0.00, except for that at pH 3.0, indicating good stability during the first 3 h of storage. The CI of the emulsions at pH 7.0 – 11.0 increased gradually with the prolonged storage time, indicating that the stability of emulsions decreased with the storage time. In addition, the CI of the emulsions at pH 3.0 was significantly greater than that of other emulsions during the whole storage ($p < 0.05$). At 28 days, CI increased with pH in the range of pH 5.0 – 11.0, indicating that the stability of emulsions decreased with the increasing pH. The degree of phase separation increased with increasing pH values due to the increased dissolution of CMCD-ODA particles in the high-pH solution [52].

The CI of the emulsions at pH 5.0 remained 0.00 during 28 days of storage. Thus, the optimum condition for emulsion stabilization was pH 5.0. As demonstrated by the rheological results, at pH 5.0, the superior viscosity and viscoelasticity of CMCD-ODA facilitated the formation of a stronger gel-network structure, which could resist the strain stress produced by the deformation of droplet and prevent the coalescence of droplet, thereby improving the stability of the emulsion system [53]. Furthermore, the hydrophobic interaction of the alkyl chains of CMCD-ODA affected the CMCD-ODA-mediated fibrillary network generated across the aqueous continuous phase, thereby enhancing the viscoelasticity of the entire emulsion phase [23]. Hence, the network formed by CMCD-ODA at pH 5.0 in the continuous phase appeared to fully covered oil droplets in the Pickering emulsions together with strong electrostatic repulsion (−46.87 mV), and this prevented the macroscopic oil phase separation, resulting in a highly stable emulsion system at pH 5.0 [31]. In this experiment, the CMCD-ODA emulsions under alkaline conditions showed a strong electrostatic repulsion that inhibited droplet flocculation and helped to improve stability, but the decrease in viscosity and viscoelasticity led to an unstable network structure. Therefore, stability could be influenced by changes in steric hindrance and electrostatic interactions in the emulsions [30]. Cui et al. also found that the stability of the system depended on the combined action of steric hindrance and electrostatic repulsion, and stability was maintained for the balance between these interactions [54].

Table 3
Creaming index of CMCD-ODA Pickering emulsions at different pH values after different storage times (3 h – 28 days) at 25 °C.

pH values	Creaming index (%)			
	3 h	7 day	14 day	28 day
3.0	9.19 ± 1.05 a	45.55 ± 0.98 a	44.37 ± 0.91 a	46.66 ± 1.27 a
5.0	0.00 b	0.00 d	0.00 d	0.00 d
7.0	0.00 b	0.00 d	0.00 d	10.46 ± 0.81 e
9.0	0.00 b	6.25 ± 0.26 c	11.50 ± 0.82 c	15.94 ± 0.43 c
11.0	0.00 b	10.12 ± 0.51 b	14.75 ± 1.65 b	20.01 ± 0.78 b

Note: Values are presented as mean ± standard deviation ($n = 3$). Different letters in the same column indicate statistical significance differences ($p < 0.05$).

3.6. Morphology and microstructure of CEO-loaded curdlan emulsions

The morphology of the CMCD-ODA emulsions stabilized at pH 5.0 was observed via CLSM. As shown in Fig. 6, the CEO phase displayed red fluorescence after dyeing with Nile red and appeared as individual oil droplets, with sphere-shaped loading in the interior of the droplets according to the merged images (Fig. 6C and F). The CMCD-ODA particles displayed green fluorescence after dyeing with Nile blue, and the Nile blue images indicated that the amphiphilic curdlan polymer might have been absorbed at the O/W interface, forming a packed layer on the droplet boundary [55]. High-magnification CLSM images were shown in Fig. 6D and E, CMCD-ODA might form a viscoelastic film around the oil droplet surface through the hydrophobic interaction between the alkyl chain in the polymer and the oil phase, which was confirmed in the merged images (Fig. 6F, the light green contour surrounding the oil droplets) [1]. This result indicated that most of CMCD-ODA might be located on the oil-water interfaces by hydrophobic interaction, resulting in a strict barrier against coalescence and maintaining the emulsions' long-term stability [52].

SEM was employed to analyze the distribution of amphiphilic curdlan on the surface of droplets and the spatial structure of the polymerized styrene beads (Fig. 6). The SEM images revealed that the droplets were sphere-shaped with a uniform droplet size distribution. The droplet size of all emulsions were < 20 μm, which verified the droplet size of the emulsion at pH 5.0 determined with the SLS method. Furthermore, a bridging structure between adjacent droplets and the thin film flakes on the surface of the microspheres were found in the high-magnification SEM images of the CMCD-ODA emulsions (Figs. 6 H and 6I), which could be contributed to improve system stability [4]. In short, the O/W Pickering emulsion fabricated by the amphiphilic self-assembly of CMCD-ODA formed a continuous network structure, which provided steric hindrance to prevent the droplets from contacting and coalescing, thereby improving the stability of the emulsions [55].

3.7. Antioxidant activity of CEO-loaded CMCD-ODA emulsions

The DPPH scavenging capacity of CEO (1 mg/mL) at pH 3.0 – 11.0 after different storage times was investigated. As shown in Fig. 7A and D, pH exhibited a great impact on the antioxidant capacity of the CEO. After 3 h of storage, the antioxidant capacity of CEO at pH 3.0 – 11.0 ranged from 76.47 % to 88.59 %, and the CEO at pH 5.0 showed the best antioxidant capacity (88.59 %). After 28 days of storage, the antioxidant capacity of CEO under pH 5.0 – 9.0 decreased slightly. However, the antioxidant capacity of CEO decreased sharply at pH 3.0 (38.44 %) and pH 11.0 (45.04 %) after 28 days of storage. This indicated that the active components of CEO were destroyed under strong acid and alkali conditions, but were stable at pH 5.0 – 9.0. After the CEO encapsulated by CMCD-ODA polymer at pH 5.0 – 9.0, the antioxidant capacity decreased slightly with the prolongation of storage time (Fig. 7A). However, the antioxidant capacity of the emulsion decreased significantly at pH 3.0 and pH 11.0 after 28 days of storage, which was related to the instability of the emulsion at pH 3.0 and pH 11.0. These results suggested that the free CEO was stable at pH 5.0, and the emulsions prepared at pH 5.0 could protect the antioxidant activity of essential oils from being destroyed during the storage.

The CMCD-ODA emulsion obtained at pH 5.0 was diluted with ultrapure water to obtain CEO dilutions with different concentrations of CEO, and then the DPPH scavenging capacity of the dilutions was investigated. As shown in Fig. 7B, at low concentrations of CEO (0.1 – 0.4 mg/mL), the CEO-loaded CMCD-ODA emulsions showed higher

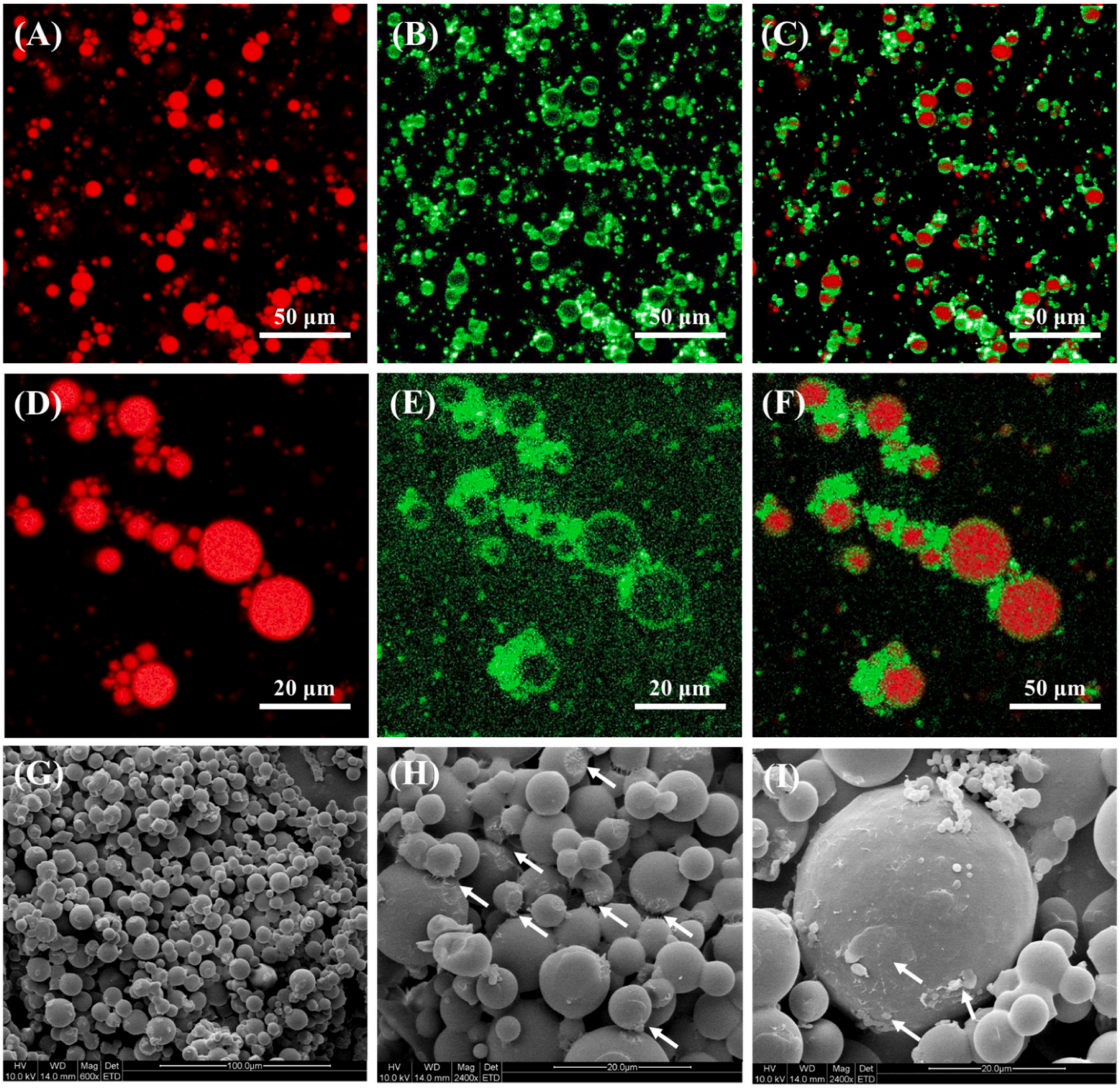

Fig. 6. CLSM and SEM images of CMCD-ODA emulsions prepared at pH 5.0.

oxidation resistance than free CEO. CEO was prone to volatilization and deterioration during the experimental process, resulting in a decrease in CEO content of the free CEO samples. However, Pickering emulsion could protect the CEO from volatilization or deterioration, making the antioxidant capacity of the emulsion higher than that of the free CEO. Conversely, under high CEO concentrations (0.8 – 1.0 mg/mL), the antioxidant capacity of the unencapsulated CEO was higher than that of the CEO-loaded CMCD-ODA emulsions. The existence of eugenol and β-caryophyllene contributed to the DPPH scavenging activity of CEO [2]. At high CEO contents, the antioxidant activity of the CEO-loaded emulsions was slightly lower than that of free CEO probably because of the interactions between the phenolic compounds in CEO and the encapsulating material [56]. Furthermore, the formation of a continuous network by the amphiphilic CMCD-ODA loading around the droplets could physically separate CEO from the free radicals, thereby reducing their interaction with free radicals [52]. However, at low CEO concentrations (0.1 – 0.4 mg/mL), the polymer concentration was also reduced after dilution, and the antioxidant capacity of emulsion was higher than that of free CEO. When the concentration of the CMCD-ODA amphiphilic polymer in the reaction system was lower than the critical aggregation concentration, the disassembled behavior of the amphiphilic curdlan derivative led to the release of CEO from the emulsions droplets. It has been reported that amphiphilic polymers can form aggregates with hydrophobic cores for loading hydrophobic components above the critical aggregation concentration, whereas the aggregates disassembled below the critical aggregation concentration [57]. Thus, the slow release of CEO from the emulsion improved the antioxidant capacity of the volatile free CEO at 0.1–0.4 mg/mL CEO concentrations.

3.8. *Antibacterial potential of CEO-loaded curdlan emulsions*

Gram-positive bacteria (*S. aureus*) and gram-negative bacteria (*E. coli*) were employed to evaluate the antibacterial capacity of the CEO emulsions. All of the CEO and CEO emulsion samples exerted a good antibacterial effect on the two tested strains (Fig. 7C). The antimicrobial activities of CEO are attributed to its primary active ingredients,

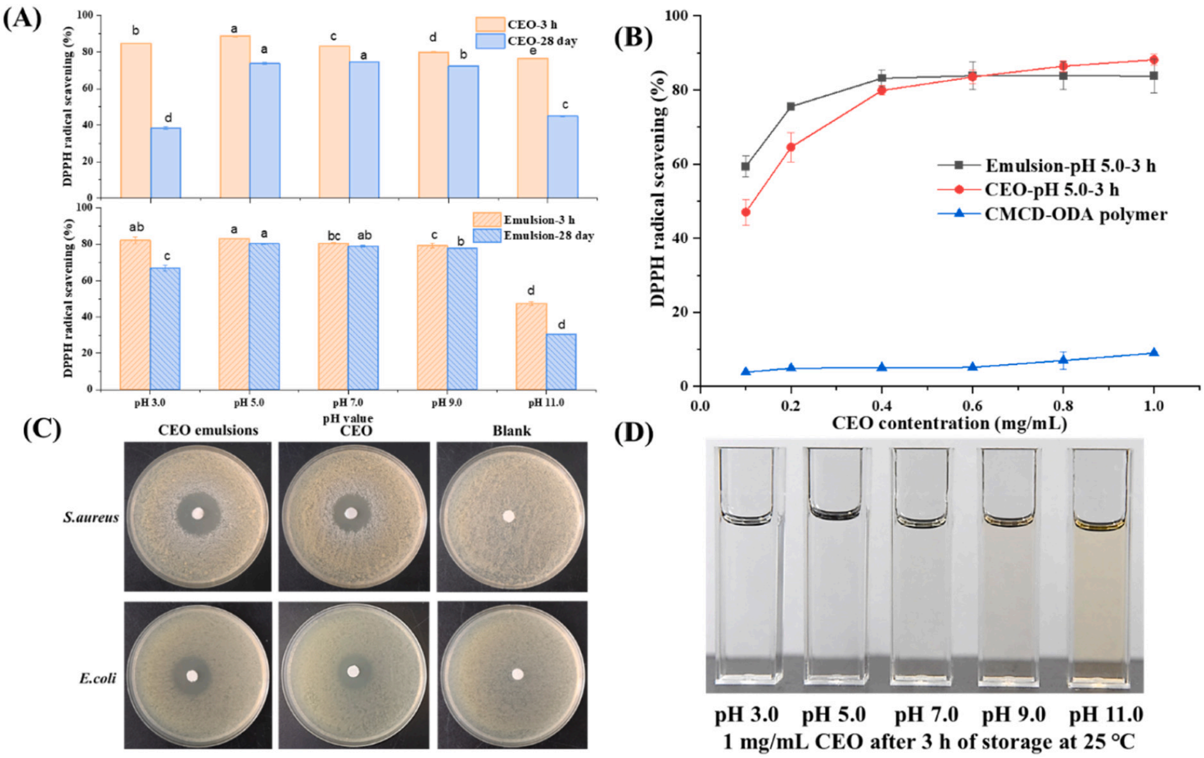

Fig. 7. (A) DPPH scavenging capacity of free CEO and CEO-loaded curdlan emulsions at different pH values after storage at 25 °C for different times (3 h/28 days). The different letters in the bars indicate significant differences ($p < 0.05$) in DPPH scavenging capacity between different pH samples at the same storage times. (B) DPPH scavenging capacity of CEO, CEO-loaded curdlan emulsions, and blank CMCD-ODA particles at different concentrations. (C) Antibacterial activity of free CEO and CEO-loaded curdlan emulsion samples. (D) Appearance of the 1 mg/mL CEO (diluted with 50 % ethanol aqueous solution) under different pH conditions after 3 h of storage at 25 °C.

including eugenol and β-caryophyllene [3]. CEO exhibits antimicrobial action possibly by penetrating through the cell membrane of the bacterium for its lipophilic characteristic then altering the permeability of the microbial membranes, resulting in the leakage of cytoplasmic contents and impaired functional properties of cells [3,56].

The inhibition zones of the CEO emulsions (2.83 cm for *S. aureus* and 2.07 cm for *E. coli*) were larger than the inhibitions zones formed by free CEO at an equivalent CEO concentration (2.70 cm for *S. aureus* and 1.87 cm for *E. coli*), indicating the improved antibacterial capacity of CEO after emulsification. This result is consistent with the higher antibacterial capacity of the CEO cellulose Pickering emulsion compared with free CEO [1]. The superior performance of the CEO-loaded CMCD-ODA emulsions compared with free CEO may be attributed to the efficient adherence to the bacterial membrane and the slow sustained release of volatile CEO from the CMCD-ODA emulsions during the experiment [1]. In addition, the volatilization or deterioration of free CEO during the antibacterial experiment also reduced its antibacterial ability.

Particularly, the CEO emulsion exhibited greater antibacterial activity in *S. aureus* than *E. coli* probably due to the different constituents of the bacteria wall. The negatively charged CMCD-ODA emulsion droplets might have self-assembled with the cell membrane of the gram-positive bacteria and facilitated the interaction with the cellular components of the bacteria, resulting in enhanced antibacterial activity [58].

4. Conclusions

An amphiphilic curdlan derivative (CMCD-ODA) was successfully synthesized by incorporating hydrophobic octadecylamine groups into CMCD. The CEO-loaded Pickering emulsion was stabilized by CMCD-ODA loading at the O/W interface. The emulsifying properties of the CMCD-ODA polymers were significantly affected by pH, and the emulsion stabilized at pH 5.0 showed the best stability with a relatively uniform size distribution during 28 days of storage. The rheological results further confirmed that the emulsions prepared at pH 5.0 exhibited superior viscosity and higher viscoelasticity than the other emulsions. The CLSM and SEM images revealed that the self-assembled CMCD-ODA polymer formed a packed layer around the oil droplets' surface and a gel network against droplet coalescence. These results suggest that emulsion stability was affected by the balance between electrostatic interaction and steric hindrance at varying pH. The CEO-loaded curdlan emulsions exhibited higher DPPH radical scavenging activity at low CEO concentrations and stronger antibacterial activity compared with the unencapsulated CEO. These findings point to an approach for enhancing the utilization efficiency of CEO and a pH-responsive emulsifier for potential application in food, hydrophobic drug delivery, and other areas.

CRediT authorship contribution statement

Huan Li: Conceptualization, Methodology, Visualization, Writing - original draft;
Chuanchao Wu: Conceptualization, Software, Visualization;
Zhongwei Yin: Writing - review & editing, Investigation;
Jianrong Wu: Conceptualization, Writing - review & editing;
Li Zhu: Methodology, Visualization, Writing-review & editing,;
Minjie Gao: Conceptualization, Investigation;
Xiaobei Zhan: Project administration, Funding acquisition, Supervision, Writing - review & editing.

Acknowledgments

This work was supported by the National Key Research and Development Program of China (grant no. 2017YFD0400302), and the

Priority Academic Program Development of Jiangsu Higher Education Institutions, the 111 Project (No. 111-2-06). Additionally, we wish to acknowledge Shanghai sanshu Biotechnology Co., LTD for their help in determination of absolute molecular weight of curdlan.

References

[1] H. Yu, G. Huang, Y. Ma, Y. Liu, X. Huang, Q. Zheng, P. Yue, M. Yang, Cellulose nanocrystals based clove oil Pickering emulsion for enhanced antibacterial activity, Int. J. Biol. Macromol. 170 (2021) 24–32.

[2] M. Hadidi, S. Pouramin, F. Adinepour, S. Haghani, S.M. Jafari, Chitosan nanoparticles loaded with clove essential oil: characterization, antioxidant and antibacterial activities, Carbohydr. Polym. 236 (2020), 116075.

[3] J. Yi, C. Gan, Z. Wen, Y. Fan, X. Wu, Development of pea protein and high methoxyl pectin colloidal particles stabilized high internal phase Pickering emulsions for β-carotene protection and delivery, Food Hydrocoll. 113 (2021), 106497.

[4] H. Dai, H. Zhang, Y. Chen, L. Ma, J. Wu, Y. Zhang, Co-stabilization and properties regulation of Pickering emulsions by cellulose nanocrystals and nanofibrils from lemon seeds, Food Hydrocoll. 120 (2021), 106884.

[5] Y. Jiang, D. Wang, F. Li, D. Li, Q. Huang, Cinnamon essential oil Pickering emulsion stabilized by zein-pectin composite nanoparticles: characterization, antimicrobial effect and advantages in storage application, Int. J. Biol. Macromol. 148 (2020) 1280–1289.

[6] X. Fang, X. Zhao, G. Yu, L. Zhang, Y. Feng, Y. Zhou, Y. Liu, J. Li, Effect of molecular weight and pH on the self-assembly microstructural and emulsification of amphiphilic sodium alginate colloid particles, Food Hydrocoll. 103 (2020), 105593.

[7] X. Zhao, F. He, G. Yu, Y. Feng, J. Li, High-viscosity Pickering emulsion stabilized by amphiphilic alginate/SiO2 via multiscale methodology for crude oil-spill remediation, Carbohydr. Polym. 273 (2021), 118492.

[8] X.B. Zhan, C.C. Lin, H.T. Zhang, Recent advances in curdlan biosynthesis, biotechnological production, and applications, Appl. Microbiol. Biotechnol. 93 (2012) 525–531.

[9] Y.B. Yu, W.D. Cai, Z.W. Wang, J.K. Yan, Emulsifying properties of a ferulic acid-grafted curdlan conjugate and its contribution to the chemical stability of beta-carotene, Food Chem. 339 (2021), 128053.

[10] Z.X. Cai, J. Wu, M. Wu, R.Q. Li, P.G. Wang, H.B. Zhang, Rheological characterization of novel carboxymethylated curdlan-silica hybrid hydrogels with tunable mechanical properties, Carbohydr. Polym. 230 (2020), 115578.

[11] J.K. Yan, H.L. Ma, X. Chen, J.J. Pei, Z.B. Wang, J.Y. Wu, Self-aggregated nanoparticles of carboxylic curdlan-deoxycholic acid conjugates as a carrier of doxorubicin, Int. J. Biol. Macromol. 72 (2015) 333–340.

[12] Y.B. Yu, M.Y. Wu, C. Wang, Z.W. Wang, T.T. Chen, J.K. Yan, Constructing biocompatible carboxylic curdlan-coated zein nanoparticles for curcumin encapsulation, Food Hydrocoll. 108 (2020), 106028.

[13] H. Li, H.T. Yang, J.J. Xu, Z.X. Gao, J.R. Wu, L. Zhu, X.B. Zhan, Novel amphiphilic carboxymethyl curdlan-based pH responsive micelles for curcumin delivery, LWT-Food Sci. Technol. 153 (2022), 112419.

[14] S.M. Rafigh, A. Vaziri Yazdi, A.A. Safekordi, A. Heydari Nasab, M. Ardjmand, F. Naderi, H. Mozafari, Protein adsorption using novel carboxymethyl-curdlan microspheres, Int. J. Biol. Macromol. 87 (2016) 603–610.

[15] T. Taubner, M. Marounek, A. Synytsya, Preparation and characterization of hydrophobic and hydrophilic amidated derivatives of carboxymethyl chitosan and carboxymethyl beta-glucan, Int. J. Biol. Macromol. 163 (2020) 1433–1443.

[16] T. Taubner, A. Synytsya, J. Copikova, Preparation of amidated derivatives of carboxymethylcellulose, Int. J. Biol. Macromol. 72 (2015) 11–18.

[17] M. Zhang, S. Asghar, X. Jin, Z. Hu, Q. Ping, Z.P. Chen, F. Shao, Y.Y. Xiao, The enhancing effect of N-acetylcysteine modified hyaluronic acid-octadecylamine micelles on the oral absorption of paclitaxel, Int. J. Biol. Macromol. 138 (2019) 636–647.

[18] A. Synytsya, M. Marounek, P. Mlčochová, S. Skoblya, H. Havlátová, P. Matějka, M. Maryška, V.R. Machovič, J. Čopíková, L. Sihelníková, N-octadecylpectinamide, a hydrophobic sorbent based on modification of highly methoxylated citrus pectin, Carbohydr. Polym. 56 (2004) 169–179.

[19] K. Huang, R. Liu, Y. Zhang, X. Guan, Characteristics of two cedarwood essential oil emulsions and their antioxidant and antibacterial activities, Food Chem. 346 (2021), 128970.

[20] J.H. Yoo, K.H. Baek, Y.S. Heo, H.I. Yong, C. Jo, Synergistic bactericidal effect of clove oil and encapsulated atmospheric pressure plasma against Escherichia coli O157:H7 and Staphylococcus aureus and its mechanism of action, Food Microbiol. 93 (2021), 103611.

[21] F.P. Gao, H.Z. Zhang, L.R. Liu, Y.S. Wang, Q. Jiang, X.D. Yang, Q.Q. Zhang, Preparation and physicochemical characteristics of self-assembled nanoparticles of deoxycholic acid modified-carboxymethyl curdlan conjugates, Carbohydr. Polym. 71 (2008) 606–613.

[22] Y. Jin, H. Zhang, Y. Yin, K. Nishinari, Comparison of curdlan and its carboxymethylated derivative by means of rheology, DSC, and AFM, Carbohydr. Res. 341 (2006) 90–99.

[23] H.M. Seo, M. Seo, K. Shin, S. Choi, J.W. Kim, Bacterial cellulose nanofibrils-armored Pickering emulsions with limited influx of metal ions, Carbohydr. Polym. 258 (2021), 117730.

[24] S. Botelho da Silva, M. Krolicka, L.A.M. van den Broek, A.E. Frissen, C.G. Boeriu, Water-soluble chitosan derivatives and pH-responsive hydrogels by selective C-6 oxidation mediated by TEMPO-laccase redox system, Carbohydr. Polym. 186 (2018) 299–309.

[25] F. Jiang, Y. Pan, D. Peng, W. Huang, W. Shen, W. Jin, Q. Huang, Tunable self-assemblies of whey protein isolate fibrils for Pickering emulsions structure regulation, Food Hydrocoll. 124 (2022), 107246.

[26] D. Qu, X.H. Huo, Z.M. Li, M. Hua, Y.S. Lu, J.B. Chen, S.S. Li, L.K. Wen, Y.S. Sun, Sediment formation and analysis of the main chemical components of aqueous extracts from different parts of ginseng roots, Food Chem. 379 (2022), 132146.

[27] V. Mikulcová, R. Bordes, A. Minařík, V. Kašpárková, Pickering oil-in-water emulsions stabilized by carboxylated cellulose nanocrystals – effect of the pH, Food Hydrocoll. 80 (2018) 60–67.

[28] Z. Wang, N. Zhang, C. Chen, R. He, X. Ju, Rapeseed protein nanogels as novel Pickering stabilizers for oil-in-water emulsions, J. Agric. Food Chem. 68 (11) (2020) 3607–3614.

[29] P.P. Wang, Z.G. Luo, C. Chun, F. Xiong, T.M. Tamer, Effects of octenyl succinic anhydride groups distribution on the storage and shear stability of Pickering emulsions formulated by modified rice starch, Carbohydr. Polym. 228 (2020), 115389.

[30] X. Zhang, B. Qi, F. Xie, M. Hu, Y. Sun, L. Han, L. Li, S. Zhang, Y. Li, Emulsion stability and dilatational rheological properties of soy/whey protein isolate complexes at the oil-water interface: influence of pH, Food Hydrocoll. 113 (2021), 106391.

[31] Y. Xie, H. Liu, Y. Li, J. Tian, X. Qin, K.I. Shabani, C. Liao, X. Liu, Characterization of Pickering emulsions stabilized by OSA-modified sweet potato residue cellulose: effect of degree of substitute and concentration, Food Hydrocoll. 108 (2020), 105915.

[32] Y. Huang, D. Zhang, Y. Zhang, H. Fang, C. Zhou, Role of ultrasound and L-lysine/L-argnine in improving the physical stability of myosin-soybean oil emulsion, Food Hydrocoll. 111 (2021), 106367.

[33] J. Buffiere, Z. Balogh-Michels, M. Borrega, T. Geiger, T. Zimmermann, H. Sixta, The chemical-free production of nanocelluloses from microcrystalline cellulose and their use as Pickering emulsion stabilizer, Carbohydr. Polym. 178 (2017) 48–56.

[34] Y. Shen, Z.J. Ni, K. Thakur, J.G. Zhang, F. Hu, Z.J. Wei, Preparation and characterization of clove essential oil loaded nanoemulsion and Pickering emulsion activated pullulan-gelatin based edible film, Int. J. Biol. Macromol. 181 (2021) 528–539.

[35] M.D.S. Campelo, E.O. Melo, S.P. Arrais, F.B.S.A.D. Nascimento, N.V. Gramosa, S.D. A. Soares, M.E.N.P. Ribeiro, C.R.D. Silva, H.V.N. Júnior, N.M.P.S. Ricardo, Clove essential oil encapsulated on nanocarrier based on polysaccharide: a strategy for the treatment of vaginal candidiasis, Colloid. Surf. A 610 (2021), 125732.

[36] Z. Alinaqi, A. Khezri, H. Rezaeinia, Sustained release modeling of clove essential oil from the structure of starch-based bio-nanocomposite film reinforced by electrosprayed zein nanoparticles, Int. J. Biol. Macromol. 173 (2021) 193–202.

[37] Z. Cai, H. Zhang, The effect of carboxymethylation on the macromolecular conformation of the (1→3)-β-D-glucan of curdlan in water, Carbohydr. Polym. 272 (2021), 118456.

[38] Y. Yu, Q. Wang, J. Yuan, X. Fan, P. Wang, L. Cui, Hydrophobic modification of cotton fabric with octadecylamine via laccase/TEMPO mediated grafting, Carbohydr. Polym. 137 (2016) 549–555.

[39] T. Xia, C. Xue, Z. Wei, Physicochemical characteristics, applications and research trends of edible Pickering emulsions, Trends Food Sci. Technol. 107 (2021) 1–15.

[40] C.G. Lopez, W. Richtering, Oscillatory rheology of carboxymethyl cellulose gels: influence of concentration and pH, Carbohydr. Polym. 267 (2021), 118117.

[41] Y. Cai, L. Huang, B. Chen, X. Zhao, M. Zhao, Q. Zhao, P. Van der Meeren, Effect of alkaline pH on the physicochemical properties of insoluble soybean fiber (ISF), formation and stability of ISF-emulsions, Food Hydrocoll. 111 (2021), 106188.

[42] H. Chen, B. Xu, C. Zhou, A.E.A. Yagoub, Z. Cai, X. Yu, Multi-frequency ultrasound-assisted dialysis modulates the self-assembly of alcohol-free zein-sodium caseinate to encapsulate curcumin and fabricate composite nanoparticles, Food Hydrocoll. 122 (2022), 107110.

[43] Z. Huang, I. Jurewicz, E. Munoz, R. Garriga, J.L. Keddie, Pickering emulsions stabilized by carboxylated nanodiamonds over a broad pH range, J Colloid Interf. Sci. 608 (2022) 2025–2038.

[44] P. Shao, H. Ma, J. Zhu, Q. Qiu, Impact of ionic strength on physicochemical stability of o/w emulsions stabilized by Ulva fasciata polysaccharide, Food Hydrocoll. 69 (2017) 202–209.

[45] Q. Liu, B. Li, Y. Li, X. Yang, C. Qiao, W. Hu, M. Liu, Solution properties of N-(2-allyl-butyl ether)-O-carboxymethyl chitosan and N-(2-allyl-isooctyl ether)-O-carboxymethyl chitosan, Int. J. Biol. Macromol. 190 (2021) 93–100.

[46] G.Q. Huang, J.X. Xiao, S.Q. Wang, H.W. Qiu, Rheological properties of O-carboxymethyl chitosan – gum arabic coacervates as a function of coacervation pH, Food Hydrocoll. 43 (2015) 436–441.

[47] X. Cai, Y. Wang, X. Du, X. Xing, G. Zhu, Stability of pH-responsive Pickering emulsion stabilized by carboxymethyl starch/xanthan gum combinations, Food Hydrocoll. 109 (2020), 106093.

[48] R.S. Hosseini, A. Rajaei, Potential Pickering emulsion stabilized with chitosan-stearic acid nanogels incorporating clove essential oil to produce fish-oil-enriched mayonnaise, Carbohydr. Polym. 241 (2020), 116340.

[49] X.M. Li, Q.T. Xie, J. Zhu, Y. Pan, R. Meng, B. Zhang, H.Q. Chen, Z.Y. Jin, Chitosan hydrochloride/carboxymethyl starch complex nanogels as novel Pickering stabilizers: physical stability and rheological properties, Food Hydrocoll. 93 (2019) 215–225.

[50] K. Yang, A. Liu, A. Hu, J. Li, Z. Zen, Y. Liu, S. Tang, C. Li, Preparation and characterization of cinnamon essential oil nanocapsules and comparison of volatile components and antibacterial ability of cinnamon essential oil before and after encapsulation, Food Control 123 (2021), 107783.

[51] N. Xiao, W. He, Y. Zhao, Y. Yao, M. Xu, H. Du, N. Wu, Y. Tu, Effect of pH and xanthan gum on emulsifying property of ovalbumin stabilized oil-in water emulsions, LWT-Food Sci. Technol. 147 (2021), 111621.

[52] M. Atarian, A. Rajaei, M. Tabatabaei, A. Mohsenifar, H. Bodaghi, Formulation of Pickering sunflower oil-in-water emulsion stabilized by chitosan-stearic acid nanogel and studying its oxidative stability, Carbohydr. Polym. 210 (2019) 47–55.

[53] M. Zhang, W. Kang, H. Yang, Z. Li, H. Zhang, F. Wang, M. Li, X. Kang, H. Jiang, A. Xie, Emulsion stabilization of cyclodextrin polymer inclusion amphiphilic polymers with different hydrophobic chain, J. Mol. Liq. 326 (2021), 115259.

[54] B. Cui, Y.M. Lu, C.P. Tan, G.Q. Wang, G.H. Li, Effect of cross-linked acetylated starch content on the structure and stability of set yoghurt, Food Hydrocoll. 35 (2014) 576–582.

[55] F. Lin, X. Zhao, S. Yang, F. He, W. Qin, H. Gong, G. Yu, Y. Feng, J. Li, Interfacial regulation and visualization of Pickering emulsion stabilized by Ca2+-triggered amphiphilic alginate-based fluorescent aggregates, Food Hydrocoll. 119 (2021), 106843.

[56] M. Radunz, M.L.M. da Trindade, T.M. Camargo, A.L. Radunz, C.D. Borges, E. A. Gandra, E. Helbig, Antimicrobial and antioxidant activity of unencapsulated and encapsulated clove (Syzygium aromaticum, L.) essential oil, Food Chem. 276 (2019) 180–186.

[57] M.J. Tizzotti, M.C. Sweedman, C. Schäfer, R.G. Gilbert, The influence of macromolecular architecture on the critical aggregation concentration of large amphiphilic starch derivatives, Food Hydrocoll. 31 (2013) 365–374.

[58] H. Majeed, F. Liu, J. Hategekimana, H.R. Sharif, J. Qi, B. Ali, Y.Y. Bian, J. Ma, W. Yokoyama, F. Zhong, Bactericidal action mechanism of negatively charged food grade clove oil nanoemulsions, Food Chem. 197 (2016) 75–83.